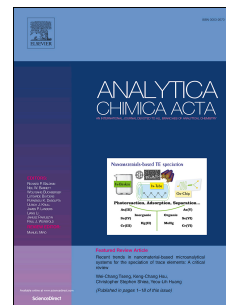


Journal Pre-proof

Controlling Serum Protein Depletion in Aqueous Biphasic Systems: Interphase Precipitation versus Bottom Phase Retention for Bisphenol A Monitoring

Maria S.M. Mendes, Inês B. Santana, Mara G. Freire, Francisca A. e Silva



PII: S0003-2670(26)00296-5

DOI: <https://doi.org/10.1016/j.aca.2026.345346>

Reference: ACA 345346

To appear in: *Analytica Chimica Acta*

Received Date: 16 December 2025

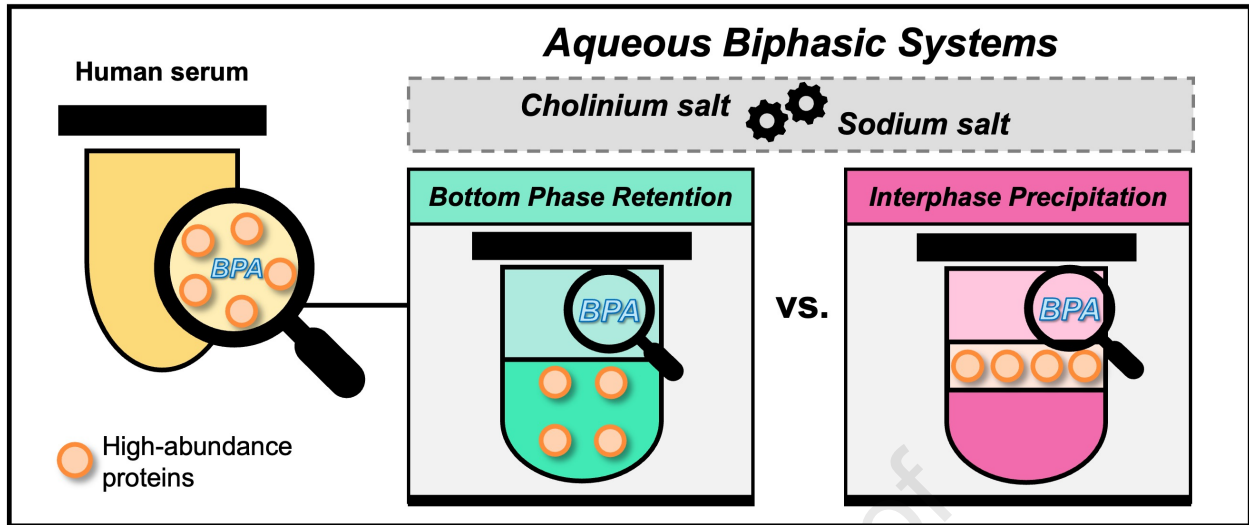
Revised Date: 2 March 2026

Accepted Date: 3 March 2026

Please cite this article as: M.S.M. Mendes, I.B. Santana, M.G. Freire, F.A. e Silva, Controlling Serum Protein Depletion in Aqueous Biphasic Systems: Interphase Precipitation versus Bottom Phase Retention for Bisphenol A Monitoring, *Analytica Chimica Acta*, <https://doi.org/10.1016/j.aca.2026.345346>.

This is a PDF of an article that has undergone enhancements after acceptance, such as the addition of a cover page and metadata, and formatting for readability. This version will undergo additional copyediting, typesetting and review before it is published in its final form. As such, this version is no longer the Accepted Manuscript, but it is not yet the definitive Version of Record; we are providing this early version to give early visibility of the article. Please note that Elsevier's sharing policy for the Published Journal Article applies to this version, see: <https://www.elsevier.com/about/policies-and-standards/sharing#4-published-journal-article>. Please also note that, during the production process, errors may be discovered which could affect the content, and all legal disclaimers that apply to the journal pertain.

© 2026 Published by Elsevier B.V.



Controlling Serum Protein Depletion in Aqueous Biphasic Systems: Interphase Precipitation versus Bottom Phase Retention for Bisphenol A Monitoring

Maria S. M. Mendes¹, Inês B. Santana¹, Mara G. Freire^{1*}, Francisca A. e Silva^{1*}

¹CICECO - Aveiro Institute of Materials, Department of Chemistry, University of Aveiro, Aveiro, Portugal

*To whom correspondence may be addressed. E-mail: maragfreire@ua.pt; francisca.silva@ua.pt

Abstract

Background: Human serum is a clinically relevant yet analytically challenging matrix. Its high abundance of proteins interferes with the detection of low-concentration biomarkers and environmental contaminants, including bisphenol A (BPA), an endocrine disruptor monitored as a marker of human exposure. High-abundance proteins introduce matrix effects that can enhance, distort or suppress analytical signals, ultimately compromising assay performance. Aqueous biphasic systems (ABS) provide a promising pretreatment strategy to address these limitations by selectively depleting high-abundance proteins and generating a cleaner matrix that supports effective analyte recovery and improved detection sensitivity.

Results: In this work, a dual-strategy ABS platform was introduced and shown to deliberately direct protein depletion via two complementary mechanisms: (i) *interphase precipitation*, where serum proteins aggregate at a solid interphase, and (ii) *bottom phase retention*, where proteins accumulate in the salt-rich bottom phase. By combining polypropylene glycol (PPG) with either cholinium or sodium salts, the salt composition tunes phase behavior, selectively depletes high-abundance proteins, and enhances BPA recovery. Sodium salts generally outperformed cholinium salts due to stronger hydration and salting-out effects. Between the two implemented strategies, systems promoting *interphase precipitation* achieved up to 94% protein depletion, while simultaneously driving BPA into the largely protein-depleted PPG-rich top phase, minimizing matrix bias and enabling more efficient detection.

Significance: This work demonstrates, for the first time, that rational control of ABS composition can selectively switch between protein precipitation and liquid-liquid partition, establishing a versatile and tunable serum pretreatment platform. This approach enables efficient depletion of high-abundance proteins and sensitive recovery of BPA and potentially other low-concentration analytes. Supported by green and blue analytical chemistry metrics, it represents a significant advance in bioanalytical workflows and environmental exposure assessment, while offering a more sustainable alternative to conventional methods.

Keywords: human serum, sample pretreatment, aqueous biphasic system, bisphenol A

1. Introduction

Human serum is a central matrix in clinical and bioanalytical studies, offering a diverse array of molecular indicators that reflect disease, exposure and physiological

46 status [1]. This molecular diversity, however, is embedded within a highly complex
47 proteome, where protein concentrations span over ten orders of magnitude [1]. High-
48 abundance proteins, predominantly human serum albumin (HSA), immunoglobulins (IgG
49 and IgA), haptoglobin, α_1 antitrypsin, and transferrin, account for nearly 85% of the total
50 serum protein content, thus shaping the behavior of the matrix [1]. As a result, low-
51 abundance analytes, including clinically and environmentally relevant markers, are
52 susceptible to suppression or masking, reducing their detectability with conventional
53 analytical methods [1].

54 Bisphenol A (BPA), an endocrine-disrupting chemical widely used in plastics and
55 resins, represents one such low-abundance analyte [2]. Its pervasive use results in
56 routine detection in human fluids, such as serum, plasma, and urine, where BPA serves
57 as a marker of exposure [2]. This concern calls for effective monitoring to assess human
58 exposure and associated health risks, including potential links to hormone-sensitive
59 cancers [2]. A range of analytical techniques, including high-performance liquid
60 chromatography (HPLC), gas chromatography-mass spectrometry (GC-MS), and
61 enzyme-linked immunosorbent assays (ELISA), have been employed for BPA
62 quantification [3]. However, because BPA typically occurs at trace concentrations
63 ($\text{ng}\cdot\text{mL}^{-1}$ or $\text{pg}\cdot\text{mL}^{-1}$), high-abundance proteins and other matrix constituents can strongly
64 interfere with its detection by introducing effects that compromise the integrity and
65 reliability of the analytical signal [3]. Consequently, efficient pretreatment is essential to
66 deplete/remove these proteins and reduce matrix bias, enabling reliable quantification
67 [3].

68 Common pretreatment strategies to support BPA detection include protein
69 precipitation (PP), solid-phase extraction (SPE) and liquid-liquid extraction (LLE) [4]. PP
70 involves the denaturation and removal of proteins using organic solvents, polymers,
71 salts, acids, bases, or heat, followed by centrifugation [4]. For instance, acetonitrile has
72 been applied as a precipitating agent, improving BPA quantification in human plasma by
73 liquid chromatography-tandem mass spectrometry (LC-MS/MS), with a reported limit of
74 detection (LOD) of about $5\text{ ng}\cdot\text{mL}^{-1}$ and a limit of quantification (LOQ) of $10\text{ ng}\cdot\text{mL}^{-1}$ [5].
75 SPE enables the isolation and concentration of target analytes from complex samples
76 through retention-elution or direct elution using a solid stationary phase, based on
77 interactions such as ion exchange, polarity, or immunoaffinity [4]. For example, SPE has
78 been successfully applied to urinary and peritoneal fluids, efficiently removing proteins
79 and enabling accurate BPA quantification by GC-MS/MS, with LODs ranging from 0.015 -
80 $0.05\text{ ng}\cdot\text{mL}^{-1}$ [6]. Finally, LLE separates compounds based on their differential solubility
81 in two immiscible phases, typically aqueous and organic [4]. BPA quantification in serum
82 by LC-MS/MS using acetonitrile as the organic phase achieved 100% recovery, with a
83 LOD of $0.009\text{ ng}\cdot\text{mL}^{-1}$ and a LOQ of $0.028\text{ ng}\cdot\text{mL}^{-1}$ [7]. Despite their effectiveness,
84 conventional methods often rely on multistep workflows and volatile or toxic solvents,
85 limiting their overall simplicity, biocompatibility, and cost-effectiveness [4]. These
86 constraints motivate the development of alternative pretreatment strategies that integrate
87 efficiency, sustainability, and analytical performance.

88 As versatile aqueous LLE platforms composed of polymers, salts, or other hydrophilic
89 compounds such as amino acids, carbohydrates and ionic liquids, aqueous biphasic
90 systems (ABS) fulfill these criteria. Their adjustable composition, combined with mild and
91 biocompatible operating conditions, enables the selective separation of diagnostic and
92 environmental markers, ultimately improving detection limits and simplifying analytical
93 workflows [8]. In urine, ABS have been used for the extraction and concentration of

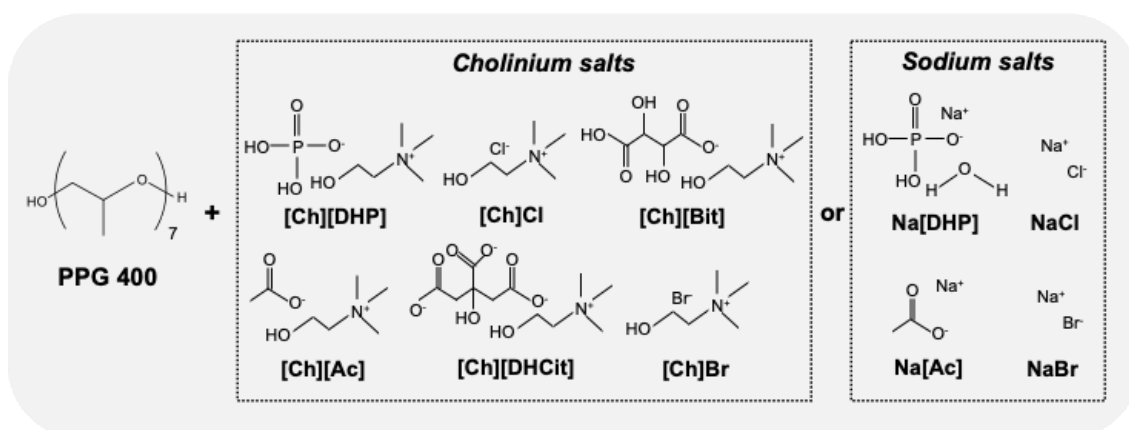
94 proteins, vitamins, drugs, and metals [9–12]. When applied to blood, these systems
95 proved compatible with various analytical techniques such as chromatography,
96 immunoassays and spectrophotometry [13–16]. In saliva, a particularly challenging
97 matrix due to analyte dilution, ABS allowed the sensitive detection of phenolic endocrine
98 disruptors, with extraction efficiencies approaching 100%, alongside substantial protein
99 depletion via interfacial precipitation [17].

100 Depending on the phase-forming components and sample matrix, ABS can be tuned
101 to operate through liquid-liquid distribution or interfacial precipitation, enabling distinct
102 separation routes for proteins and small molecules [18]. By adjusting the composition
103 and physicochemical environment, ABS can be directed toward protein solubilization or
104 aggregation, thus providing versatile and controllable tools for biological sample
105 pretreatment [19–21]. Although both mechanisms have been individually described
106 [10,13], their systematic comparison and rational exploitation as complementary routes
107 for protein depletion in ABS remain underexplored. Herein, the deliberate control of ABS
108 composition is demonstrated to selectively induce either protein precipitation or liquid-
109 liquid distribution, establishing a dual-strategy platform for improved BPA analysis in
110 human serum: (i) *bottom phase retention*, where high-abundance proteins (HSA and
111 IgG) are removed through selective accumulation in a liquid phase, and (ii) *interphase*
112 *precipitation*, where these proteins are efficiently depleted via solid-phase formation at
113 the interphase. In both strategies, BPA is preferentially extracted into the top aqueous
114 phase, ensuring compatibility with analytical detection and enabling accurate
115 quantification in protein-rich conditions. ABS were tailored by combining polypropylene
116 glycol (PPG) with either cholinium or sodium salts, where differences in hydration, ionic
117 character and interaction with proteins define phase behavior and direct the system
118 toward *interphase precipitation* or *bottom phase retention*. In addition, the analytical
119 performance and sustainability of the proposed platform were systematically evaluated
120 using green and blue analytical chemistry metrics.

122 2. Materials and methods

123 2.1. Chemicals, analytical standards, and biological samples

124
125 Polypropylene glycol with an average molecular weight of 400 g·mol⁻¹ (PPG 400;
126 Sigma-Aldrich) was used to prepare ABS in combination with selected salts. Cholinium
127 salts included cholinium dihydrogen phosphate ([Ch][DHP], purity = 98 wt%; Iolitec),
128 cholinium acetate ([Ch][Ac], purity = 98 wt%; Iolitec), cholinium dihydrogen citrate
129 ([Ch][DHCit], purity = 99 wt%; Sigma-Aldrich), cholinium bitartrate ([Ch][Bit], purity = 97
130 wt%; Acros Organics), cholinium chloride ([Ch]Cl, purity = 98 wt%; Acros Organics) and
131 cholinium bromide ([Ch]Br, purity = 98 wt%; TCI). Sodium salts comprised sodium
132 dihydrogen phosphate 1-hydrate (Na[DHP], purity = 99 wt%; PanReac AppliChem),
133 sodium acetate (Na[Ac], purity = 100 wt%; Prolabo), sodium chloride (NaCl, purity = 99.5
134 wt%; Fisher Scientific), and sodium bromide (NaBr, purity = 99 wt%; Sigma-Aldrich).
135 Chemical structures of all compounds are presented in Figure 1. Phosphate-buffered
136 saline (PBS) pellets were purchased from Sigma-Aldrich and used to prepare an
137 aqueous solution yielding 0.01 M phosphate buffer, 0.0027 M potassium chloride (KCl)
138 and 0.137 M sodium chloride (NaCl), with a pH 7.4 at 25 °C, according to the
139 manufacturer's instructions.



140
141 **Figure 1.** Chemical structures of ABS components, highlighting the polymer (PPG 400) and the
142 two salt families.
143

144 Human serum (H4522 – Lot # SLBX6353) was obtained from Sigma-Aldrich and
145 stored at $-20\text{ }^{\circ}\text{C}$ until use. The mobile phase for Size-Exclusion High-Performance Liquid
146 Chromatography (SE-HPLC) used in the quantification of IgG and HSA was prepared
147 with doubled distilled water purified by a reverse osmosis system followed by a treatment
148 with a Milli-Q plus 185 water purification system, as well as sodium dihydrogen
149 phosphate 1-hydrate ($\text{NaH}_2\text{PO}_4 \cdot \text{H}_2\text{O}$, purity = 99%), disodium hydrogen phosphate 7-
150 hydrate ($\text{Na}_2\text{HPO}_4 \cdot 7\text{H}_2\text{O}$, purity = 99%) and NaCl (purity = 99.5 %) from PanReac
151 AppliChem. Calibration curves were established using lyophilized HSA (purity > 97 wt%;
152 stored at $4\text{ }^{\circ}\text{C}$ until use; Sigma-Aldrich) and purified human IgG ($29.4\text{ mg}\cdot\text{mL}^{-1}$; stored at
153 $-80\text{ }^{\circ}\text{C}$ until use; Innovative Research, inc.).

154 For BPA quantification, the HPLC mobile phase consisted of an aqueous solution of
155 formic acid (purity = 99 wt%; Carlo Erba) and acetonitrile HPLC-grade (purity = 99.99
156 wt%; Fisher Chemical). BPA standard (purity > 99 wt%) was obtained from Sigma-
157 Aldrich.

158 2.2. ABS binodal curves

160
161 Binodal curves of ABS composed of PPG 400 and [Ch]Br, Na[DHP], NaBr, NaCl or
162 Na[Ac] were determined to identify mixture compositions within biphasic regions. These
163 results were complemented with binodal curves previously reported for PPG 400 ABS
164 containing [Ch][DHP], [Ch][Ac], [Ch][Bit], [Ch][DHCit], or [Ch]Cl [22].

165 Binodal curves were experimentally obtained using the cloud point titration method
166 at atmospheric pressure and $(25 \pm 1)\text{ }^{\circ}\text{C}$ [22]. Aqueous stock solutions of PPG 400 (90
167 wt%) and salt solutions (25-60 wt%) were prepared for this purpose. The titration
168 consisted of gradually adding the salt solution dropwise to the PPG 400 solution under
169 continuous stirring until turbidity indicated phase separation. Water was then added
170 dropwise until the mixture became clear again, corresponding to a monophasic region.
171 Repeating this procedure while weighing all added components enabled calculation of
172 mixture compositions (wt%) used to construct binodal curves.
173

174 2.3. HSA and IgG depletion

175
176 Specific compositions within ABS biphasic regions were selected to evaluate the
177 ability of different ABS to deplete IgG and HSA through either *bottom phase retention* or

178 *interphase precipitation*, as shown in Figure 2. For direct comparison, most systems were
179 prepared with 30 wt% PPG 400, 30 wt% cholinium or sodium salt, 38 wt% PBS aqueous
180 solution, and 2 wt% human serum. However, for ABS containing sodium salts with lower
181 aqueous solubility (NaBr, Na[Ac], NaCl, Na[DHP]), the composition was adjusted to 30
182 wt% PPG 400, 15 wt% sodium salt, 53 wt% PBS aqueous solution, and 2 wt% human
183 serum. It should be noted that PBS solution was included as the aqueous component to
184 complete 100 wt% of each ABS composition. Consequently, its content varies between
185 38 and 53 wt%, depending on the specific polymer-salt pair. PBS aqueous solution also
186 provides a consistent ionic background and physiologically relevant conditions, reducing
187 uncontrolled effects on system behavior.

188 All components except human serum were weighed and vortex-mixed until
189 completely dissolved. Human serum was then added to reach a final ABS mass of 1.00 g,
190 comprising 0.30 g of PPG 400, 0.02 g of human serum, and either 0.30 g or 0.15 g of
191 salt combined with 0.38 g or 0.53 g of PBS aqueous solution, depending on the
192 composition. The mixtures were centrifuged at 3500 rpm for 10 min, and phases were
193 carefully separated using syringes. All ABS assays were performed in triplicate to allow
194 reporting of mean values and standard deviations. In all cases, the top phase was
195 enriched in PPG 400, whereas the bottom phase was enriched in the cholinium or
196 sodium salt. When present, the solid interphase corresponded to the precipitated high-
197 abundance proteins.

198 Each aqueous phase and the initial human serum samples were analyzed by SE-
199 HPLC using a Chromaster HPLC system (Hitachi) equipped with a Shodex Protein KW-
200 802.5 analytical column (8 mm × 300 mm) and a Shodex Protein KW-G 6B guard column.
201 The mobile phase (50 mM of NaH₂PO₄·H₂O/Na₂HPO₄·7H₂O buffer and 0.3 M NaCl) was
202 run isocratically at 0.5 mL·min⁻¹ for 40 min. The injection volume was 25 μL, with protein
203 detection at 280 nm using a diode-array detector (DAD). Column oven and autosampler
204 temperatures were maintained at 25 °C and 10 °C, respectively. HSA and IgG
205 concentrations in the top and bottom phases were quantified using calibration curves
206 previously established in the range 0.01-1.0 mg·mL⁻¹. The corresponding calibration
207 curves, including the coefficient of determination (R^2), limits of detection (LOD), limits of
208 quantification (LOQ), and relative standard deviations (RSD, %), are shown in Figure S1
209 in the Supplementary Material. The LOD was calculated from calibration curves analyzed
210 in duplicate using the ratio between the standard error of the regression (sy/x) and the
211 slope of the calibration curve, multiplied by a factor of 3.3. The LOQ was subsequently
212 estimated as three times the corresponding LOD value. The RSD (%) was calculated as
213 the ratio of the standard deviation to the mean of replicate measurements at each
214 concentration, multiplied by 100, and is reported as a concentration-dependent interval.

215 The direct isolation and analysis of the solid interphase were technically challenging
216 with the type of systems here studied, increasing the risk of cross-contamination and
217 analytical errors. Therefore, protein content at the interphase was calculated by mass
218 balance from the measured protein amounts in the two liquid phases and the initial serum
219 content.

220 Because the two ABS depletion strategies rely on distinct separation mechanisms,
221 i.e., protein precipitation at a solid interphase or protein retention in the bottom liquid
222 phase, the efficiency of protein depletion was expressed uniformly as recovery yield
223 ($RY_{\text{IgG/HSA}}\%$; Equation 1), defined as:
224

$$RY_{IgG/HSA}\% = \frac{m_{IgG/HSA}^{Top/Inter/Bottom}}{m_{IgG/HSA}^{Serum}} \times 100 \quad (1)$$

226

227 where $m_{IgG/HSA}^{Top/Inter/Bottom}$ corresponds to the mass of IgG or HSA quantified in the
 228 respective phase (top, interphase or bottom), and $m_{IgG/HSA}^{Serum}$ is the initial mass of each
 229 protein in the commercial serum. This approach allows direct comparison of protein
 230 distribution across all phases, regardless of whether depletion occurs via *interphase*
 231 *precipitation* or *bottom phase retention*.

232

233 2.4. BPA recovery and analytical performance

234

235 ABS that exhibited the best performance in depleting high-abundance proteins were
 236 subsequently evaluated for their ability to extract BPA into the protein-depleted top
 237 phase. This phase contains markedly reduced levels of HSA and IgG due to their
 238 depletion either by *interphase precipitation* or by *bottom phase retention* (Figure 2).
 239 Spiked human serum was prepared by adding BPA to a final concentration of 0.3 mg·mL⁻¹.
 240 1, a value selected according to the sensitivity range of the HPLC-DAD. It should be
 241 noted that testing BPA levels higher than typical biological concentrations is useful, as it
 242 is representative of BPA partition in ABS, while allowing verification that the PPG-rich
 243 phase is not saturated. Spiked samples were further incorporated into ABS following the
 244 same preparation and phase-separation procedure used for protein depletion assays.

245

246 Each top phase was analyzed by Reverse-Phase High-Performance Liquid
 247 Chromatography (RP-HPLC) using a Shimadzu HPLC system equipped with a Kinetex®
 248 C18 LC column (250 x 4.6 mm) and a DAD detector. The mobile phase, consisting of
 249 0.002% v/v formic acid in water (A) and acetonitrile (B) was delivered at 1 mL·min⁻¹ for
 250 45 min under the following gradient: 0-3 min, 80% A / 20% B; 4-6 min, 65% A / 35% B;
 251 20-28 min, 45% A / 55% B; 33-45 min, 80% A / 20% B. The injection volume was 25 µL,
 252 the detection wavelength was set at 230 nm and the column oven was maintained at 30
 253 °C. BPA quantification was performed using a calibration curve constructed from
 254 standard solutions (0.01-1.0 mg·mL⁻¹) prepared under the initial conditions of the
 255 gradient elution method, i.e., acetonitrile/water with 0.002% v/v formic acid (v/v, 20/80).
 256 The corresponding calibration curve, including the R^2 (0.9994), LOD (0.049 mg·mL⁻¹),
 257 LOQ (0.15 mg·mL⁻¹) and RSD (0-4%), is shown in Figure S1 in the Supplementary
 258 Material.

259

260 To assess potential matrix effects arising from the presence of PPG 400 during BPA
 261 quantification, a calibration curve was prepared in the PPG-rich top phase of the ABS
 262 composed of 30 wt% PPG 400, 30 wt% NaBr and 40 wt% PBS aqueous solution (cf.
 263 Figure S2 in the Supplementary Material). Comparison of the calibration curves yielded
 264 a slope ratio of 1.04, confirming negligible matrix interference across the working
 265 concentration range.

266

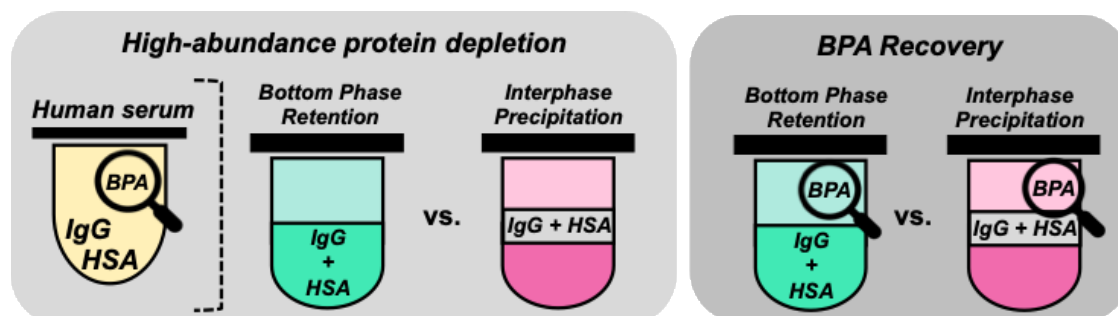
267 To evaluate analytical performance, recovery yields of BPA ($RY_{BPA}\%$, Equation 2)

268

$$RY_{BPA}\% = \frac{m_{BPA}^{Top}}{m_{BPA}^{Serum}} \times 100 \quad (2)$$

269

269 where m_{BPA}^{Top} is the mass of BPA in the top phase, and m_{BPA}^{Serum} is the initial mass added
 270 to the serum sample.
 271



272
 273 **Figure 2.** Control of ABS composition to achieve either *interphase precipitation* or *bottom phase*
 274 *retention* of high-abundance proteins, enabling protein depletion in human serum and BPA
 275 recovery from spiked samples.
 276

276

277 3. Results and Discussion

278 This work establishes an ABS-design framework for protein depletion in human
 279 serum, demonstrating a dual-strategy approach in which phase behavior is strategically
 280 manipulated to induce either liquid-liquid protein distribution or interfacial protein
 281 precipitation. These behaviors were explored to enhance analytical detection of low-
 282 abundance analytes, here represented by BPA, by selectively removing high-abundance
 283 serum proteins that compromise sensitivity and accuracy. BPA was selected as a model
 284 analyte due to its health and environmental relevance, as well as the analytical
 285 challenges it poses in protein-rich matrices. The ABS pretreatment strategy, though
 286 developed for BPA, is anticipated to be applicable to other low-concentration analytes.

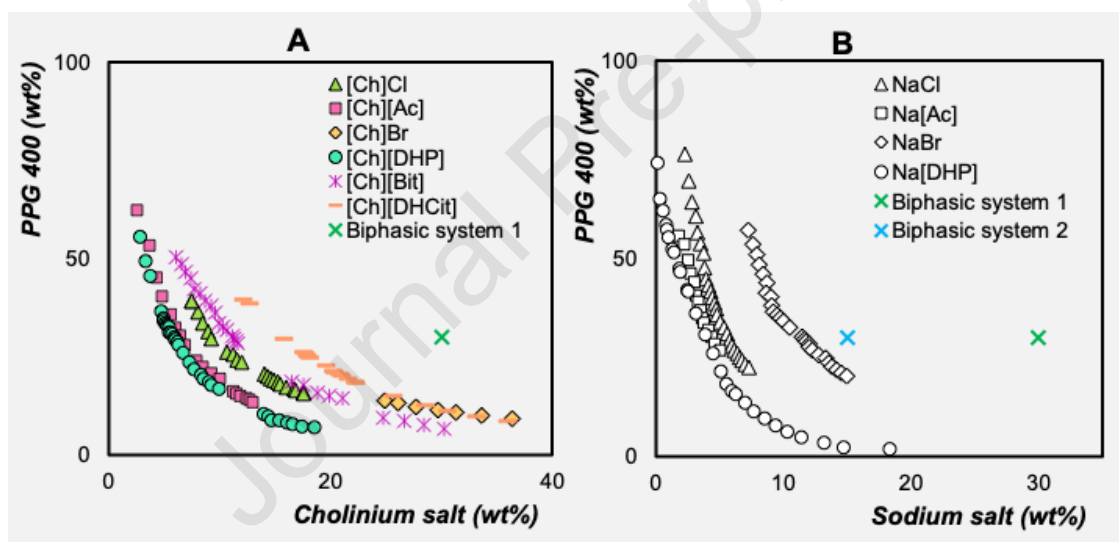
287 To implement this design strategy, cholinium and sodium salts were systematically
 288 compared as phase-forming agents in combination with PPG 400. PPG 400 was
 289 selected due to its well-balanced physicochemical properties, namely its intermediate
 290 hydrophilic-hydrophobic character and high-water miscibility, which together promote
 291 efficient phase formation with both sodium and cholinium salts [22]. These features
 292 enable rapid phase separation and efficient mass transfer, which are particularly
 293 beneficial for analytical workflows [23]. Moreover, the combination of PPG 400 with
 294 different salts allows for deliberate tuning of ABS hydrophilicity, salting-out strength
 295 and molecular interactions. These parameters are critical for driving protein depletion
 296 toward either *bottom phase retention* or *interphase precipitation*: the two complementary serum
 297 pretreatment strategies identified in this work (Figure 2). Specifically, cholinium salts
 298 were chosen for their biocompatibility, tunable hydrophilicity, and capacity to tailor
 299 molecular interactions, while sodium salts were included as classical agents capable of
 300 promoting efficient phase separation through well-defined ion-water interactions [24,25].
 301 For the present work, these compounds are referred to as “cholinium salts” to maintain
 302 consistency with the designation of sodium salts, while they are commonly featured in
 303 ionic liquids studies. Using salts systematically varied in both anion and cation type
 304 enabled a mechanistic evaluation of the contributions of each ionic component to phase
 305 behavior and sample pretreatment. By comparing systems in which either the anion or
 306 the cation was held constant, it became possible to separate anion-driven from cation-
 307 driven effects, enabling a more rational design of phase formation and protein depletion
 308 strategies.

309

310 **3.1. Controlling ABS phase separation via ionic selection**

311

312 With ABS-design rationale now delineated, the influence of ionic composition on ABS
 313 formation and the resulting binodal curves, which define the operational window for
 314 inducing protein depletion, was first examined. Cholinium salts shared a common cation,
 315 but incorporated different anions (viz. [Ch][DHP], [Ch][Ac], [Ch]Cl, [Ch][Bit], [Ch][DHCit],
 316 and [Ch]Br), whereas the sodium salts included matched anions (viz. Na[DHP], Na[Ac],
 317 NaBr, and NaCl) to enable direct comparison. With most systems containing cholinium
 318 salts previously reported [22], ABS containing [Ch]Br and sodium salts were
 319 experimentally characterized here to extend the understanding of ion specific effects.
 320 The corresponding binodal curves are presented in Figure 3, demarcating the boundary
 321 between monophasic and biphasic regions, with compositions above the curve forming
 322 two immiscible aqueous phases. The closer the curve is to the origin, the more efficient
 323 the ionic species in promoting phase separation, and the broader the compositional
 324 window available for designing protein depletion strategies. Numerical binodal data for
 325 the newly characterized systems are detailed in the Supplementary Material (Table S1).
 326



327

328 **Figure 3.** Binodal curves for ABS comprising PPG 400 with various (A) cholinium and (B) sodium
 329 salts, showing biphasic system compositions selected for protein depletion and BPA recovery
 330 studies. Data obtained experimentally or from literature [22].

331

332 Among cholinium salts (Figure 3A), ABS formation is strongly anion-dependent,
 333 with higher water-affinity anions more effectively excluding PPG 400 and promoting
 334 phase separation. This behavior, well-documented in previous studies [22], is
 335 exemplified by [Ch][DHP], followed by [Ch][Ac], [Ch]Cl, [Ch][Bit] and [Ch]Br. [DHP]⁻ anion
 336 possessing the highest polar surface, accounts for [Ch][DHP]'s superior phase-
 337 separation ability. Both [Ac]⁻ and Cl⁻ act as strong hydrogen bond acceptors, efficiently
 338 interacting with water and favoring phase separation in the presence of relatively
 339 hydrophobic polymers such as PPG 400 [22,26]. [Ch][Bit], derived from a dicarboxylic
 340 acid, contains additional hydroxyl groups and a longer alkyl chain compared to [Ac]⁻,
 341 which modulates water interactions and slightly reduces its ability to induce phase
 342 separation [22]. [Ch]Br, experimentally characterized in this work for the first time,
 343 exhibits lower water affinity than [Ch]Cl, resulting in reduced capacity to exclude PPG

344 400 and form ABS [22,26]. [Ch][DHCit], despite its high-water affinity, behaves as an
345 outlier, likely due to self-aggregation events that impede homogeneous phase separation
346 [22]. Overall, water-cholinium salt interactions dominate these systems, with additional
347 contributions from cholinium salt-polymer interactions in specific cases.

348 According to Figure 3B, sodium salts present an analogous anion-mediated
349 profile, with ABS formation efficiency following the order $\text{Na}[\text{DHP}] > \text{Na}[\text{Ac}] > \text{NaCl} >$
350 NaBr . In polymer-salt systems, phase separation is predominantly governed by the
351 salting-out effect, whereby ion hydration promotes the exclusion of PPG 400 into a
352 distinct aqueous phase [27–29]. Sodium salts generally form ABS more efficiently than
353 cholinium salts, due to smaller cations, higher charge density, and stronger ionic
354 interactions [30]. High-charge-density ions drive liquid-liquid demixing by displacing
355 PPG, reducing its solubility and enhancing phase separation [31]. In contrast, cholinium-
356 salt ABS depend on a broader interplay among PPG 400, the salt, and water, with the
357 cholinium cation forming additional interactions, especially hydrogen bonds, that may
358 moderate phase separation compared with sodium salts [22]

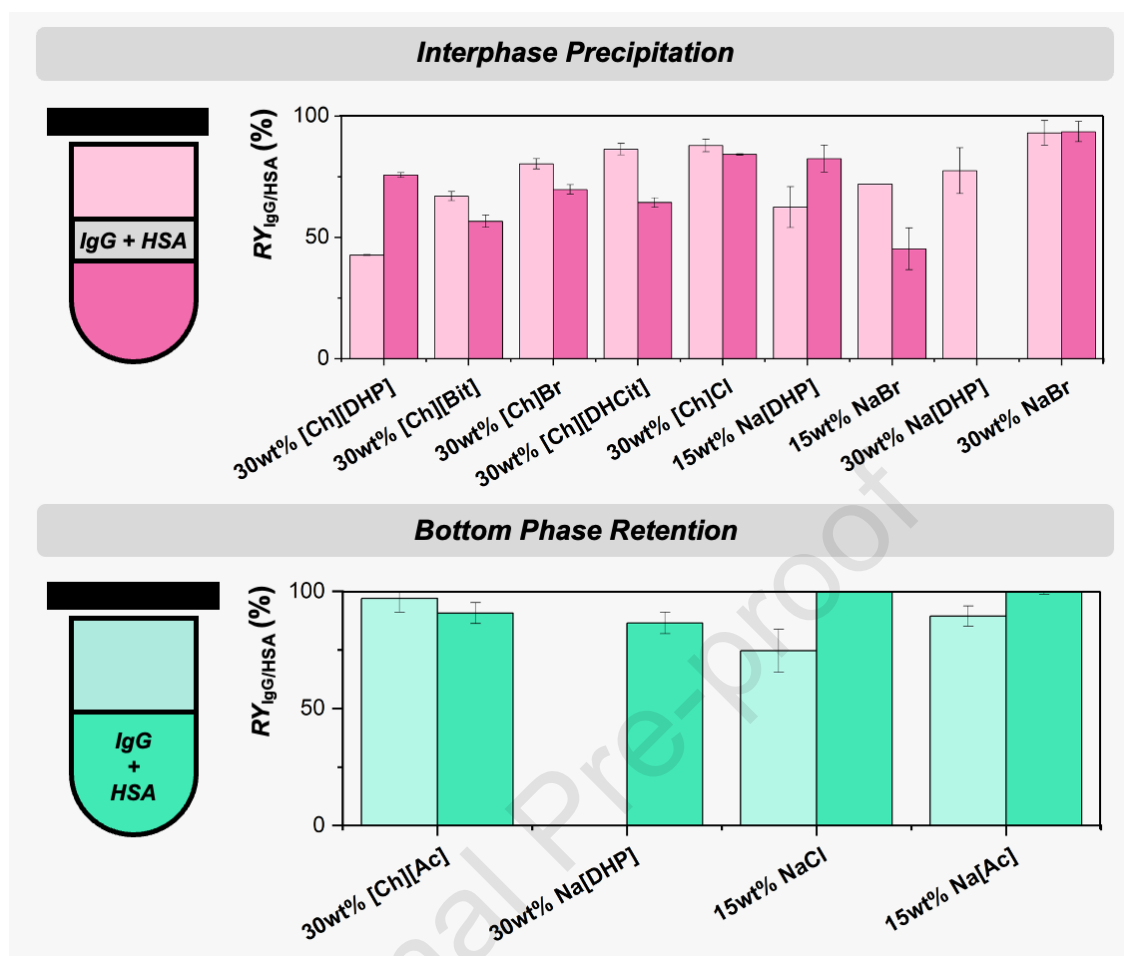
359

360 **3.2. Tailoring protein depletion in human serum via ABS: *interphase*** 361 ***precipitation vs. bottom phase retention***

362 Supported by each ABS binodal curves, representative biphasic mixture
363 compositions were selected to investigate HSA and IgG depletion from human serum. In
364 Figure 3, biphasic system 1 (30 wt% PPG 400, 30 wt% cholinium or sodium salt, 38 wt%
365 PBS aqueous solution, and 2 wt% human serum) represents the standard mixture used
366 for most salts, enabling direct comparison. Biphasic system 2 (15 wt% NaBr, Na[Ac] or
367 NaCl) was selected for salts with lower aqueous solubility to ensure stable two-phase
368 formation while maintaining 30 wt% PPG 400 and 2 wt% serum, with the salt and PBS
369 aqueous solution contents adjusted accordingly. These formulations allowed the
370 assessment of protein depletion under consistent preparation conditions while
371 accounting for the solubility limitations of each salt.

372 Protein recovery yields in the phase of interest are shown in Figure 4 for PPG 400
373 ABS tuned with cholinium or sodium salts, revealing the combined effects of ion
374 hydration and specific interactions with the proteins. The results further highlight the two
375 complementary depletion strategies: *interphase precipitation*, where high-abundance
376 proteins aggregate at the interface between the phases, and *bottom phase retention*,
377 where proteins preferentially accumulate in the salt-rich liquid phase. Representative
378 photographs of both behaviors are provided in the Supplementary Material (Figure S3),
379 and detailed numerical data for all systems, including recoveries in the other phases, are
380 provided in Table S2. Depending on ionic composition and ABS formation capacity,
381 these results demonstrate how ABS can be tailored to control serum fractionation and
382 reduce matrix complexity.

383



384

385

386

387

388

389

390

391

392

393

394

395

396

397

398

399

400

401

402

403

404

405

406

407

Figure 4. Recovery yields of IgG (RY_{IgG} , light bars) and HSA (RY_{HSA} , dark bars) in the interphase (pink bars), and bottom phase (green bars) of ABS comprising 30 wt% PPG 400, 15-30 wt% cholinium or sodium salt, 53-38 wt% PBS aqueous solution and 2 wt% human serum. Green bars indicate *bottom phase retention*, pink bars denote *interphase precipitation*, and the left-side schematic illustrates the corresponding protein depletion strategy visually. Values are expressed as mean \pm standard deviation ($n = 3$).

Interphase precipitation was predominant in systems containing PPG 400 combined with 30 wt% [Ch][DHP], [Ch][Bit], [Ch]Br, [Ch][DHCit], [Ch]Cl, and 15-30 wt% Na[DHP] or NaBr (Figure 4, pink bars). These systems readily form ABS, facilitating protein destabilization and aggregation at the interphase, with IgG depletion ranging from 43% to 93% and HSA depletion from 13% to 94%. The high concentration and relative hydrophobicity of PPG in the top phase exclude water, destabilizing proteins and promoting aggregation [32]. The salts further enhance this effect by modulating protein hydration and solubility through ionic interactions and water-structuring forces [33]. This combined effect ultimately promotes protein precipitation at the interphase, with the salting-out effect particularly relevant for the sodium salts. Moreover, comparisons between cholinium and sodium salts with the same anion reveal protein-specific behaviors. In the Na[DHP]/[Ch][DHP] pair, the sodium salt showed higher efficiency in IgG depletion (77% vs. 43%), whereas the cholinium salt was more effective for HSA depletion (76% vs. 13%). For the NaBr/[Ch]Br pair, the sodium salt outperformed the cholinium salt in both IgG (93% vs. 80%) and HSA (94% vs. 70%) depletion. These differences arise from the higher charge density, smaller size, and stronger hydration of

408 Na⁺, promoting aggregation via salting-out, while cholinium cations form stabilizing
409 interactions that maintain protein solubility [9,22,34,35]. Additionally, increasing the salt
410 concentration enhances the salting-out effect, as observed for NaBr, where IgG and HSA
411 depletion improved significantly at 30 wt% compared to 15 wt% [34]. Protein-specific
412 interactions, including electrostatic forces and hydrophobic effects, also modulate
413 retention and precipitation [34], as exemplified by the contrasting HSA response to
414 Na[DHP] concentration (15 wt%: 82% vs. 30 wt%: 13%).

415 *Bottom phase retention* was observed in systems containing NaCl, Na[Ac], and
416 [Ch][Ac] in combination with PPG 400 (Figure 4, green bars). In these systems, proteins
417 accumulate in the salt-rich bottom phase due to strong hydrogen bond accepting ability
418 of [Ac]⁻ and Cl⁻ anions, reducing protein solubility in the polymer-rich top phase [29,36].
419 Among these, the [Ch][Ac] system achieved depletion of 97% for IgG and 91% for HSA,
420 revealing the strong hydrophilic interactions between the cholinium salt and water that
421 enhance phase separation [36]. Sodium salts also demonstrated effective protein
422 depletion, with Na[Ac] achieving 89% IgG and 100% HSA depletion, and NaCl achieving
423 75% IgG and 100% HSA depletion, closely matching the performance of the [Ch][Ac]
424 system.

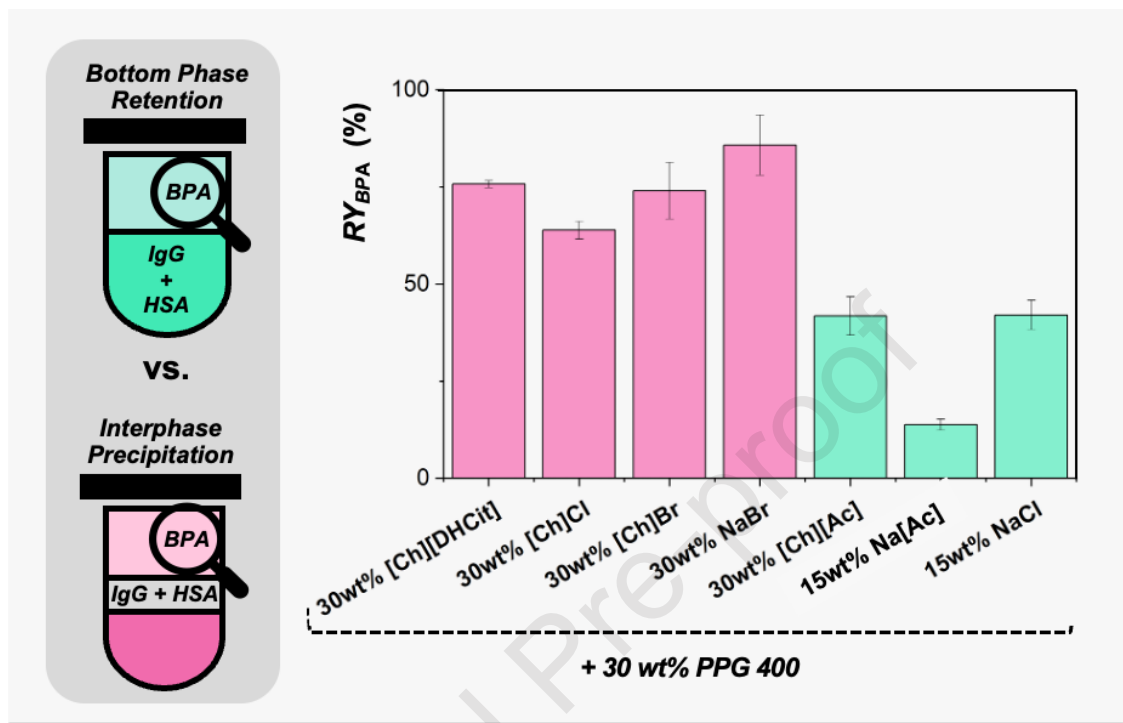
425 Of note, at 30 wt% Na[DHP], HSA mainly accumulates into the bottom phase,
426 whereas IgG precipitates at the interphase (both behaviors are reflected in Figure 4, with
427 bottom phase and interphase recoveries indicated by the green and pink bars,
428 respectively). This observation demonstrates that adjusting ABS composition and the
429 ionic component allows different proteins to undergo either *interphase precipitation* or
430 *bottom phase retention* within the same system. Under these conditions, the larger size
431 and multimeric structure of IgG likely render it more susceptible to salting-out and
432 interphase precipitation, whereas the smaller size of HSA could favor its retention in
433 solution [37]. This highlights the potential of ABS as a versatile platform that could be
434 tailored to the characteristics of diverse biological matrices and molecular targets as well
435 as to specific analytical requirements of the intended applications.

436 Overall, the observed protein depletion behaviors can be rationalized based on
437 the specific ionic properties of each system. *Interphase precipitation* is driven by
438 polymer-induced protein destabilization, amplified by ionic interactions and salting-out
439 effects. In turn, *bottom phase retention* relies on ion hydration and reduced protein
440 solubility in the polymer-rich phase. Protein depletion was most efficient in systems
441 containing 30 wt% [Ch][DHCit], [Ch]Cl, [Ch]Br, or NaBr for *interphase precipitation*, and
442 in systems containing 30 wt% of [Ch][Ac], 15 wt% Na[Ac], or 15 wt% NaCl for *bottom*
443 *phase retention*. The best-performing systems were comparable for IgG removal
444 between *interphase precipitation* (93% IgG and 94% HSA with 30 wt% NaBr) and *bottom*
445 *phase retention* (97% IgG and 91% HSA with 30 wt% [Ch][Ac]), whereas *bottom phase*
446 *retention* proved superior for HSA depletion, achieving complete removal with 15 wt%
447 Na[Ac] or NaCl. The resulting protein-depleted matrices provide an ideal environment to
448 evaluate the recovery and analytical performance in BPA analysis.

449 3.3. Assessing BPA in protein-depleted ABS phases

451
452 Following the targeted removal of high-abundance serum proteins, the most
453 efficient ABS from each depletion strategy were evaluated for their ability to recover BPA.
454 This approach enables assessment of analytical performance in a simplified, protein-
455 depleted matrix, minimizing interference from HSA and IgG and providing a clearer

456 insight into BPA recovery and detection accuracy. Figure 5 presents the recovery yields
 457 of BPA in the PPG-rich top phase for each system; detailed data is given in the
 458 Supplementary Material (Table S3).
 459
 460



461
 462 **Figure 5.** Recovery yield of BPA (RY_{BPA}) in the top phase of ABS comprising 30 wt% PPG 400,
 463 15-30 wt% cholinium or sodium salt, 53-38 wt% PBS aqueous solution and 2 wt% human serum
 464 spiked with $0.3 \text{ mg}\cdot\text{mL}^{-1}$ of BPA. Green bars indicate *bottom phase retention*, pink bars denote
 465 *interphase precipitation*, and the left-side schematic illustrates the corresponding protein
 466 depletion strategy visually. Values are expressed as mean \pm standard deviation ($n = 3$).
 467

468 In systems where proteins were predominantly removed via *interphase*
 469 *precipitation*, BPA was recovered in the top, polymer-rich phase. This preferential
 470 migration is facilitated by the hydrophobic characteristics of BPA (logarithm of the
 471 octanol-water partition coefficient, $\log K_{o/w} = 3.32$), favoring its partition to the less polar,
 472 PPG-rich phase [38]. The effective precipitation of high-abundance proteins at the
 473 interphase further reduces potential interactions with BPA, creating a favorable migration
 474 environment for analyte enrichment. Among these systems, the recovery of BPA reached
 475 up to 86%, highlighting the synergy between protein depletion and analyte recovery.
 476 Among tested salts, the superior performance of NaBr can be attributed to its strong ionic
 477 strength [39], which promotes efficient salting-out.

478 Conversely, in systems dominated by *bottom phase retention*, BPA recovery in
 479 the top phase was markedly lower (14-42%), irrespective of the salt. The retention of
 480 proteins in the bottom phase suggests a competitive migration environment that
 481 disfavors BPA migration toward the polymer-rich top phase. The association of BPA with
 482 the protein-rich bottom phase may be driven by hydrophobic effects or other non-
 483 covalent forces, which stabilize its retention alongside the proteins [40]. These findings
 484 suggest that macromolecular composition and intermolecular interactions critically
 485 influence BPA behavior in ABS.

486 Remarkably, ABS protein depletion not only simplifies the serum matrix but also
487 critically influences the subsequent recovery of BPA. The *interphase precipitation*
488 strategy demonstrates superior efficiency, simultaneously enabling selective protein
489 depletion (93% of IgG and 94% of HSA) and preferential BPA top phase recovery (86%)
490 in a single step, with ABS composed of 30 wt% PPG 400 and 30 wt% NaBr. In RP-HPLC
491 coupled with UV detection, high-abundance proteins can interfere with analyte signals,
492 causing peak broadening, baseline noise, and co-elution [41], ultimately compromising
493 quantification accuracy and sensitivity. Accordingly, the chromatographic profiles
494 obtained after ABS pretreatment, together with the blank PPG 400 top phase
495 chromatogram with no BPA, support the clean-up efficiency and confirm that the
496 polymer-rich phase does not interfere with BPA determination (cf. Figure S4 in the
497 Supplementary Material). By efficiently removing high-abundance proteins, ABS could
498 reduce matrix interference, sharpen analyte peaks, and enhance detection reliability,
499 representing a clear advantage over untreated serum samples.

500 In addition to matrix clean-up, the possibility of analyte preconcentration
501 contributes to the analytical versatility of the ABS platform. In this context, BPA
502 concentration in the PPG-rich phase provides insight into its enrichment capability. To
503 this aim, Table S4 in the Supplementary Material reports the masses of the ABS phases,
504 measured BPA concentrations, and the calculated maximum enrichment (EF_{max}) and
505 concentration (CF) factors for the *interphase precipitation* strategy, which provided the
506 highest BPA recovery. In an initial assessment, EF_{max} , expressed as the ratio of total
507 ABS mass to PPG-rich phase mass, ranged from 3.35 to 5.19, reflecting the theoretical
508 concentration achievable from phase mass reduction. However, CF , the ratio of actual
509 BPA concentration in the PPG-rich phase to the initial serum concentration, remained
510 below 0.1, despite the high recovery yield (64-86%). This behavior reflects phase volume
511 effects related to the PPG-rich phase relative to the amount of serum incorporated into
512 the ABS. While the system could be technically adjusted for preconcentration, in its
513 current form it primarily serves for matrix clean-up through protein depletion rather than
514 analyte enrichment.

515 Beyond methodological benefits, BPA recovery holds practical potential for a
516 variety of applications. In environmental biomonitoring, trace BPA levels in human serum
517 could be concentrated to detectable levels, assisting epidemiological studies and
518 exposure assessments [42]. In clinical toxicology, where low-level BPA exposure may
519 impact endocrine function, reliable quantification could be achieved even in complex
520 matrices, facilitating patient monitoring [43]. In this context, future efforts could explore
521 the application of this approach to real human serum samples, further reinforcing its
522 translational potential. Finally, ABS could also be applied in food safety and
523 pharmacokinetic studies, where the accurate measurement of trace BPA in diverse types
524 of biological samples is required [44]. Such versatility enables more sensitive and reliable
525 monitoring of BPA exposure across protein-rich matrices and varied real-world
526 scenarios, with clear implications for human health and environmental safety.

527 528 **3.4. Sustainability assessment of the ABS-HPLC-DAD method for BPA** 529 **monitoring**

530
531 To evaluate the environmental sustainability of the proposed ABS-HPLC-DAD
532 method for human serum pretreatment and BPA recovery, complementary green and

533 blue metrics were applied. The Analytical GREENness Metric (AGREE) [45] and
534 AGREEprep [46] were used to assess the greenness of the overall analytical procedure
535 and the sample preparation step, respectively, based on the principles of “Green
536 Analytical Chemistry” and “Green Sample Preparation”. Both metrics are presented as
537 color-coded circular diagrams, where each segment represents a criterion and is colored
538 from green (most sustainable) to red (least sustainable), with a central numerical score
539 ranging from 0 to 1. A more detailed evaluation of sample pretreatment sustainability
540 was assisted by the Sample Preparation Metric of Sustainability (SPMS), considering
541 key parameters related to reagent consumption, procedural complexity, energy demand,
542 and waste generation [47]. SPMS results are displayed as a clock-style diagram with
543 color-coded squares and a central numeric score from 0 to 10, allowing rapid visual
544 assessment of performance. Method applicability and practicality were further assessed
545 using the Blue Applicability Grade Index (BAGI), which evaluates attributes associated
546 with throughput, instrumentation, automation, and operational simplicity [48]. BAGI
547 results are shown as an asteroid pictogram with a central score, enabling straightforward
548 comparison of method practicality. The results of the applied metrics are compiled in
549 Figure 6.
550

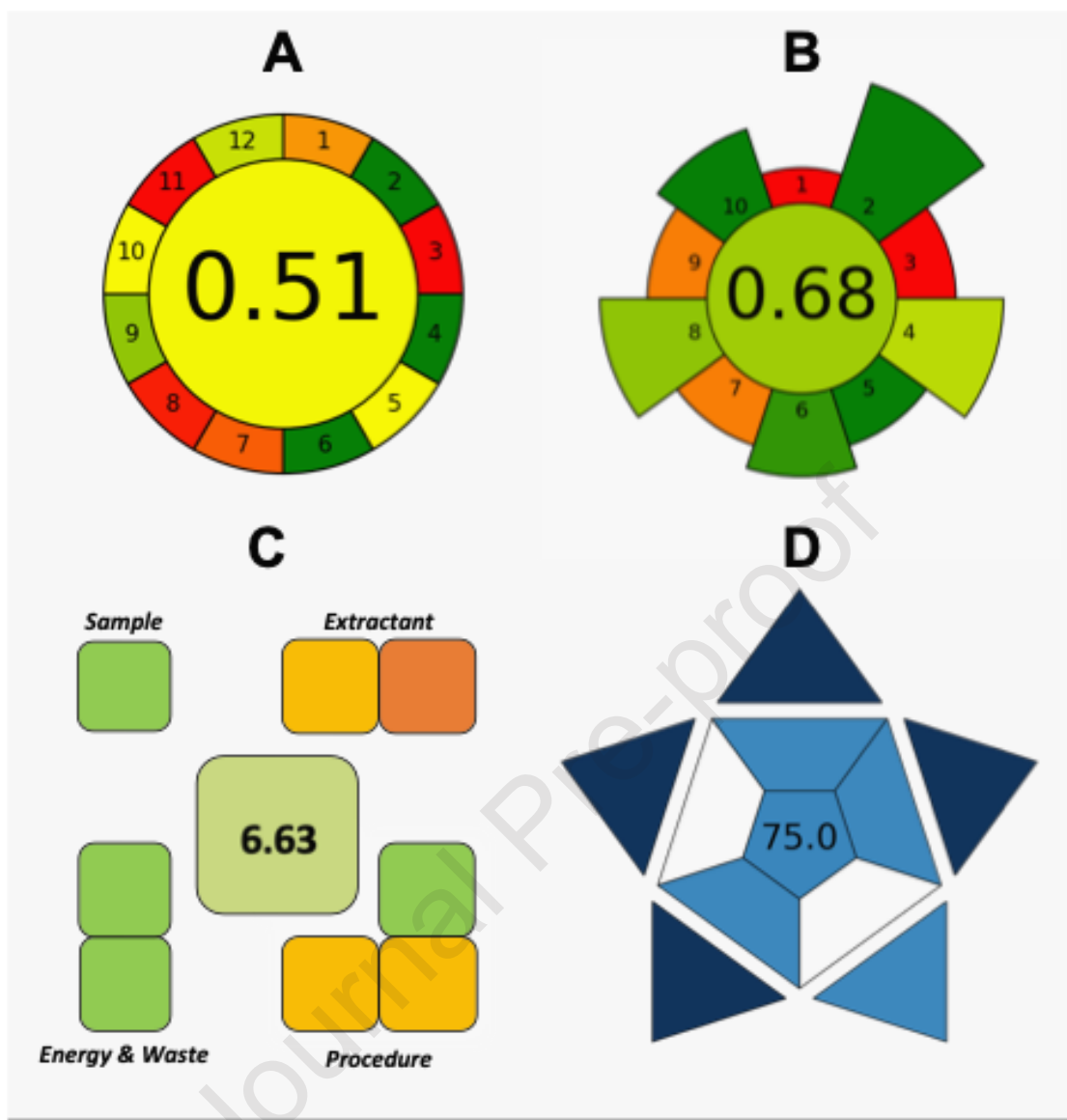


Figure 6. Evaluation of the proposed ABS-HPLC-DAD method by green and blue analytical metrics: (A) AGREE, (B) AGREEprep, (C) SPMS and (D) BAGI.

According to AGREE (Figure 6A), the proposed method achieved a global score of 0.51, indicating a moderate overall greenness. Favorable scores were obtained for criteria related to integration (protein depletion and BPA extraction in a single ABS step), avoidance of derivatization and the use of a miniaturized sample preparation system (1 g total mass) and minimal sample amount (~0.02 g). Additional positive contributions arise from operation at room temperature, and the partial use of safe, low-toxicity reagents (PPG 400 and cholinium or sodium salts). In contrast, lower scores were assigned to criteria related to direct analysis and *in situ* measurement, highlighting the need for off-line sample pretreatment, as well as to analytical waste generation and reagent toxicity, mainly resulting from the chromatographic analysis step, which requires extended HPLC run times and the use of acetonitrile.

The AGREEprep evaluation (Figure 6B) yielded an overall score of 0.68 for the ABS pretreatment step. High scores were observed for the use of safer, non-volatile aqueous solutions of PPG and salts, minimal serum consumption (~0.02 g per ABS), process integration (simultaneous protein depletion and BPA extraction), and operator

570 safety. Intermediate scores were assigned to sample throughput and energy
571 consumption, reflecting single-sample processing and the centrifugation step, while
572 waste minimization received a moderate score due to aqueous/polymer streams. The
573 post-preparation chromatographic analysis contributed to a lower score, consistent with
574 the inherent energy and resource demands of HPLC.

575 To further refine the evaluation of the sample preparation step, the SPMS was
576 applied (Figure 6C), yielding a score of 6.63. High performance was associated with low
577 sample and extractant volumes, a limited number of steps, room-temperature operation,
578 and the absence of derivatization. However, SPMS penalizes the lack of extractant
579 reusability, centrifugation-based separation, and limited throughput, preventing the
580 method from achieving higher scores. Finally, the practical applicability assessed by
581 BAGI (Figure 6D) resulted in a score of 75. Strengths include standard instrumentation,
582 commercially available reagents, and straightforward operations, while lower scores
583 arise from the ABS pretreatment involving centrifugation, manual handling, and limited
584 automation, which constrain throughput.

585 Overall, the ABS-HPLC-DAD method achieves a balanced performance,
586 combining moderate-to-good greenness, efficient and integrated sample preparation,
587 and practical applicability, while highlighting areas for further optimization such as
588 throughput, extractant reusability, and automation.

589

590 **3.5. Benchmarking the ABS-HPLC-DAD method against reported BPA analysis** 591 **approaches**

592

593 To contextualize the performance of the proposed ABS-HPLC-DAD method, its
594 analytical performance and sustainability aspects were compared with reported methods
595 for BPA quantification in biological samples. Comparison criteria are provided in Table
596 S5 in the Supplementary Material, including sample pretreatment strategies, analytical
597 techniques, extraction times, and limits of detection [5–7,49,50]. The corresponding
598 AGREE, AGREEprep, SPMS, and BAGI scores are summarized in Figure S5 in the
599 Supplementary Material.

600 Conventional sample pretreatment strategies for BPA extraction, such as PP,
601 SPE, and LLE using volatile organic solvents, have been widely reported. Examples
602 include acetonitrile-induced PP in human plasma with an LOD of 5 ng·mL⁻¹ [5], SPE
603 followed by GC-MS/MS achieving LODs as low as 0.05 ng·mL⁻¹ in urine [6], and
604 acetonitrile-based LLE coupled to LC-MS/MS providing an LOD of 0.009 ng·mL⁻¹ in
605 human serum [7]. While these approaches deliver excellent analytical sensitivity, their
606 sustainability is limited by multistep workflows, extensive use of volatile organic solvents,
607 derivatization, increased waste generation and energy-intensive procedures, such as
608 centrifugation, evaporation, and filtration, as indicated by AGREE and AGREEprep
609 scores (Figure S5 in the Supplementary Material). These factors are also reflected in
610 lower SPMS values and only moderate BAGI scores, indicating reduced green
611 credentials and limited applicability for high-throughput or routine analysis.

612 More recent approaches based on ABS composed of ionic liquids (IL-ABS) [49]
613 and LLE comprising hydrophobic eutectic solvents (HES) [50] represent advances
614 toward greener sample pretreatment. IL-ABS applied to urine samples allowed BPA
615 extraction with UV-Vis detection, but prolonged equilibration times (up to 720 min)
616 restricted sample throughput and reduced AGREEprep and SPMS scores [49]. HES-
617 based pretreatment of whole blood, coupled to LC-MS/MS, decreased volatile organic

618 solvent use and shortened preparation to ~30 min [49]. Despite improved solvent
619 sustainability, reliance on sonication, centrifugation and energy-intensive LC-MS/MS
620 instrumentation limits overall practicality and negatively impacted AGREE and BAGI
621 scores.

622 Remarkably, the proposed ABS-HPLC-DAD method achieves intermediate-to-
623 high scores across AGREE (0.51), AGREEprep (0.68), SPMS (6.63), and BAGI (75),
624 reflecting a deliberate compromise between analytical sensitivity, environmental
625 sustainability, and operational practicality. However, the reported LOD of 49000 ng·mL⁻¹
626 is higher than those obtained by MS-based methods [5–7], which is expected due to
627 the use of DAD instead of MS/MS. Even so, the method avoids derivatization, reduces
628 solvent toxicity, minimizes energy consumption, and relies on widely available HPLC
629 equipment, enhancing accessibility for routine analysis. Compared with conventional
630 pretreatment strategies, ABS offer a favorable balance of features: cost-effectiveness,
631 small reagent volumes, energy efficiency (no repeated centrifugation or evaporation),
632 eco-friendliness (aqueous phases instead of volatile solvents), and analytical
633 performance, combining efficient protein depletion with BPA recovery in a single step (up
634 to 86%). While previously reported methods may excel in analytical sensitivity, the ABS
635 strategy provides a holistic improvement across key “Green Sample Preparation”
636 metrics, highlighting its potential for sustainable analytical workflows [51].

637

638 4. Conclusions

639

640 This work establishes a dual-strategy ABS serum pretreatment platform,
641 exploiting cholinium and sodium salts with PPG 400 to selectively deplete high-
642 abundance proteins. Two complementary strategies were identified using ABS, with the
643 choice of salt determining which approach is implemented: *interphase precipitation*, in
644 which proteins aggregate at the interphase, and *bottom phase retention*, where proteins
645 accumulate in the salt-rich bottom phase. Following protein depletion, the PPG-rich top
646 phase served as the primary medium for BPA recovery and accurate detection,
647 benefiting from reduced protein interference.

648 Protein depletion was strongly dependent on ABS ionic composition. *Interphase*
649 *precipitation*, driven by polymer-induced protein destabilization and enhanced by ionic
650 interactions and salting-out effects, achieved up to 94% depletion of IgG and HSA in
651 systems containing [Ch][DHCit], [Ch]Cl, [Ch]Br, or NaBr. *Bottom phase retention*, relying
652 on ion hydration and the reduced solubility of proteins in the polymer-rich phase, reached
653 97% IgG and 100% HSA depletion in systems with [Ch][Ac], Na[Ac], or NaCl. These
654 optimized systems yielded a simplified, protein-depleted matrix, allowing assessment of
655 BPA recovery and analytical performance, which were markedly influenced by the
656 protein depletion strategy. The *interphase precipitation* strategy clearly excelled, as the
657 effective depletion of high-abundance proteins from the bulk phases (93% of IgG and
658 94% of HSA) allowed BPA to be predominantly recovered into the PPG-rich top phase,
659 with minimal losses (86% recovery).

660 The environmental sustainability and practical applicability of the proposed ABS-
661 HPLC platform were critically assessed using complementary green and blue analytical
662 metrics. The intermediate-to-high scores obtained confirm that the method achieves a
663 balanced compromise between analytical performance, environmental sustainability,
664 and operational feasibility, outperforming previously reported approaches.

665 By exploring mechanistically distinct protein depletion routes in ABS, this work
666 demonstrates how ionic composition and phase design can be tailored to control protein
667 distribution, minimize matrix interferences, and maximize analyte recovery. This dual-
668 strategy platform provides an adaptable and streamlined framework for serum
669 pretreatment and the selective enrichment of exposure markers and potentially other
670 biomarkers. Ultimately, it offers a sustainable and efficient route to improve analytical
671 accuracy in exposure assessment and environmental monitoring, while also holding
672 relevance for broader bioanalytical applications, including clinical analysis.

673

674 **CRedit authorship contribution statement**

675

676 **Maria S. M. Mendes:** Methodology, Validation, Formal analysis, Investigation, Data
677 Curation, Writing-original draft, Visualization; **Inês B. Santana:** Formal analysis,
678 Investigation, Data Curation; **Mara G. Freire:** Conceptualization, Funding Acquisition,
679 Supervision, Writing – review & editing; **Francisca A. e Silva:** Conceptualization, Writing
680 – review & editing, Supervision, Funding Acquisition, Project Administration.

681

682 **Acknowledgements**

683

684 This work was developed within the scope of the project CICECO – Aveiro Institute of
685 Materials, UID/50011/2025 (DOI 10.54499/UID/50011/2025) & LA/P/0006/2020 (DOI
686 10.54499/LA/P/0006/2020), financed by national funds through the FCT/MCTES
687 (PIDDAC). This work was supported by national funds (OE) through FCT/MCTES under
688 the project ILSurvive, PTDC/EMD-TLM/3253/2020 (DOI 10.54499/PTDC/EMD-
689 TLM/3253/2020). M.S.M.M. acknowledges FCT for the doctoral grant 2022.11229.BD
690 (DOI 10.54499/2022.11229.BD). F.A.eS. acknowledges FCT for the researcher contract
691 CEECIND/03076/2018/CP1559/CT0024 (DOI
692 10.54499/CEECIND/03076/2018/CP1559/CT0024) under the Scientific Employment
693 Stimulus – Individual Call 2018.

694

695 **Declaration of competing interest**

696

697 The authors declare that they have no known competing financial interests or personal
698 relationships that could have appeared to influence the work reported in this paper.

699

700 **Data availability**

701

702 Data will be made available on request.

703

704 **References**

705

706 [1] E. Bellei, S. Bergamini, E. Monari, L.I. Fantoni, A. Cuoghi, T. Ozben, A. Tomasi,
707 High-abundance proteins depletion for serum proteomic analysis: concomitant
708 removal of non-targeted proteins, *Amino Acids* 40 (2011) 145–156.
709 <https://doi.org/10.1007/s00726-010-0628-x>.

710 [2] L.N. Vandenberg, M. V. Maffini, C. Sonnenschein, B.S. Rubin, A.M. Soto,
711 Bisphenol-A and the Great Divide: A Review of Controversies in the Field of

- 712 Endocrine Disruption, *Endocr. Rev.* 30 (2009) 75–95.
713 <https://doi.org/10.1210/er.2008-0021>.
- 714 [3] N. Caballero-Casero, L. Lunar, S. Rubio, Analytical methods for the determination
715 of mixtures of bisphenols and derivatives in human and environmental exposure
716 sources and biological fluids. A review, *Anal. Chim. Acta* 908 (2016) 22–53.
717 <https://doi.org/10.1016/j.aca.2015.12.034>.
- 718 [4] P.L. Kole, G. Venkatesh, J. Kotecha, R. Sheshala, Recent advances in sample
719 preparation techniques for effective bioanalytical methods, *Biomedical
720 Chromatography* 25 (2011) 199–217. <https://doi.org/10.1002/bmc.1560>.
- 721 [5] I.A. Wiraagni, M.A. Mohd, R. bin Abd Rashid, D.E. bin M. Haron, Validation of a
722 simple extraction procedure for bisphenol A identification from human plasma,
723 *PLoS One* 14 (2019) e0221774. <https://doi.org/10.1371/journal.pone.0221774>.
- 724 [6] A. Simonelli, R. Guadagni, P. De Franciscis, N. Colacurci, M. Pieri, P. Basilicata,
725 P. Pedata, M. Lamberti, N. Sannolo, N. Miraglia, Environmental and occupational
726 exposure to bisphenol A and endometriosis: urinary and peritoneal fluid
727 concentration levels, *Int. Arch. Occup. Environ. Health* 90 (2017) 49–61.
728 <https://doi.org/10.1007/s00420-016-1171-1>.
- 729 [7] K. Owczarek, P. Kubica, B. Kudłak, A. Rutkowska, A. Konieczna, D. Rachoń, J.
730 Namieśnik, A. Wasik, Determination of trace levels of eleven bisphenol A
731 analogues in human blood serum by high performance liquid chromatography–
732 tandem mass spectrometry, *Science of The Total Environment* 628–629 (2018)
733 1362–1368. <https://doi.org/10.1016/j.scitotenv.2018.02.148>.
- 734 [8] M.S.M. Mendes, M.E. Rosa, F. Ramalho, M.G. Freire, F.A. e Silva, Aqueous two-
735 phase systems as multipurpose tools to improve biomarker analysis, *Sep. Purif.
736 Technol.* 317 (2023) 123875. <https://doi.org/10.1016/j.seppur.2023.123875>.
- 737 [9] T. Trtić-Petrović, A. Dimitrijević, N. Zdolšek, J. Đorđević, A. Tot, M. Vraneš, S.
738 Gadžurić, New sample preparation method based on task-specific ionic liquids for
739 extraction and determination of copper in urine and wastewater, *Anal. Bioanal.
740 Chem.* 410 (2018) 155–166. <https://doi.org/10.1007/s00216-017-0705-z>.
- 741 [10] Z. Du, Y.L. Yu, J.H. Wang, Extraction of proteins from biological fluids by use of
742 an ionic liquid/aqueous two-phase system, *Chemistry - A European Journal* 13
743 (2007) 2130–2137. <https://doi.org/10.1002/chem.200601234>.
- 744 [11] M.G. Bogdanov, I. Svinjarov, Analysis of acetylcholinesterase inhibitors by
745 extraction in choline saccharinate aqueous biphasic systems, *J. Chromatogr. A*
746 1559 (2018) 62–68. <https://doi.org/10.1016/j.chroma.2018.01.007>.
- 747 [12] P. Berton, R.P. Monasterio, R.G. Wuilloud, Selective extraction and determination
748 of vitamin B12 in urine by ionic liquid-based aqueous two-phase system prior to
749 high-performance liquid chromatography, *Talanta* 97 (2012) 521–526.
750 <https://doi.org/10.1016/j.talanta.2012.05.008>.
- 751 [13] M.E. Rosa, M.S.M. Mendes, E. Carmo, J.P. Conde, J.A.P. Coutinho, M.G. Freire,
752 F.A. e Silva, Tailored pretreatment of serum samples and biomarker extraction
753 afforded by ionic liquids as constituents of aqueous biphasic systems, *Sep. Purif.
754 Technol.* 322 (2023) 124248. <https://doi.org/10.1016/j.seppur.2023.124248>.
- 755 [14] W. Yu, K. Li, Z. Liu, H. Zhang, X. Jin, Novelty aqueous two-phase extraction
756 system based on ionic liquid for determination of sulfonamides in blood coupled
757 with high-performance liquid chromatography, *Microchemical Journal* 136 (2018)
758 263–269. <https://doi.org/10.1016/j.microc.2017.03.053>.

- 759 [15] A. Gong, X. Zhu, Surfactant/ionic liquid aqueous two-phase system extraction
760 coupled with spectrofluorimetry for the determination of dutasteride in
761 pharmaceutical formulation and biological samples, *Fluid Phase Equilib.* 374
762 (2014) 70–78. <https://doi.org/10.1016/j.fluid.2014.04.022>.
- 763 [16] J. Flieger, A. Czajkowska-Żelazko, Aqueous two phase system based on ionic
764 liquid for isolation of quinine from human plasma sample, *Food Chem.* 166 (2015)
765 150–157. <https://doi.org/10.1016/j.foodchem.2014.06.037>.
- 766 [17] R. González-Martín, F.A. e Silva, M.J. Trujillo-Rodríguez, D. Díaz Díaz, J.
767 Lorenzo-Morales, M.G. Freire, V. Pino, Ionic liquid-based aqueous biphasic
768 systems as one-step clean-up, microextraction and preconcentration platforms for
769 the improved determination of salivary biomarkers, *Green Chemistry* 25 (2023)
770 8544–8557. <https://doi.org/10.1039/d3gc02046k>.
- 771 [18] J.A. Asenjo, B.A. Andrews, Aqueous two-phase systems for protein separation: A
772 perspective, *J. Chromatogr. A* 1218 (2011) 8826–8835.
773 <https://doi.org/10.1016/j.chroma.2011.06.051>.
- 774 [19] M. Iqbal, Y. Tao, S. Xie, Y. Zhu, D. Chen, X. Wang, L. Huang, D. Peng, A. Sattar,
775 M.A.B. Shabbir, H.I. Hussain, S. Ahmed, Z. Yuan, Aqueous two-phase system
776 (ATPS): an overview and advances in its applications, *Biol. Proced. Online* 18
777 (2016) 1–18. <https://doi.org/10.1186/s12575-016-0048-8>.
- 778 [20] E.C. Antunes, H. Temmink, B. Schuur, Polymer and alcohol-based three-phase
779 partitioning systems for separation of polysaccharide and protein, *Journal of*
780 *Chemical Technology & Biotechnology* 99 (2024) 259–269.
781 <https://doi.org/10.1002/jctb.7534>.
- 782 [21] G.M. Rather, M.N. Gupta, Three phase partitioning leads to subtle structural
783 changes in proteins, *Int. J. Biol. Macromol.* 60 (2013) 134–140.
784 <https://doi.org/10.1016/j.ijbiomac.2013.05.018>.
- 785 [22] M. V. Quental, M. Caban, M.M. Pereira, P. Stepnowski, J.A.P. Coutinho, M.G.
786 Freire, Enhanced extraction of proteins using cholinium-based ionic liquids as
787 phase-forming components of aqueous biphasic systems, *Biotechnol. J.* 10 (2015)
788 1457–1466. <https://doi.org/10.1002/biot.201500003>.
- 789 [23] C.A. Suarez Ruiz, O. Cabau-Peinado, C. van den Berg, R.H. Wijffels, M.H.M.
790 Eppink, Efficient Fractionation of Lipids in a Multiproduct Microalgal Biorefinery by
791 Polymers and Ionic Liquid-Based Aqueous Two-Phase Systems, *ACS Sustain.*
792 *Chem. Eng.* 10 (2022) 789–799.
793 <https://doi.org/10.1021/acssuschemeng.1c06017>.
- 794 [24] P.P. Madeira, V.N. Uversky, B.Y. Zaslavsky, Effects of Inorganic Salts on Phase
795 Separation in Aqueous Solutions of Poly(ethylene glycol), *Int. J. Mol. Sci.* 26
796 (2025) 4545. <https://doi.org/10.3390/ijms26104545>.
- 797 [25] M. Petkovic, J.L. Ferguson, H.Q.N. Gunaratne, R. Ferreira, M.C. Leitão, K.R.
798 Seddon, L.P.N. Rebelo, C.S. Pereira, Novel biocompatible cholinium-based ionic
799 liquids—toxicity and biodegradability, *Green Chemistry* 12 (2010) 643.
800 <https://doi.org/10.1039/b922247b>.
- 801 [26] A.F.M. Cláudio, L. Swift, J.P. Hallett, T. Welton, J.A.P. Coutinho, M.G. Freire,
802 Extended scale for the hydrogen-bond basicity of ionic liquids, *Physical Chemistry*
803 *Chemical Physics* 16 (2014) 6593. <https://doi.org/10.1039/c3cp55285c>.
- 804 [27] X. Zhao, X. Xie, Y. Yan, Liquid–liquid equilibrium of aqueous two-phase systems
805 containing poly(propylene glycol) and salt ((NH₄)₂SO₄, MgSO₄, KCl, and KAc):

- 806 experiment and correlation, *Thermochim. Acta* 516 (2011) 46–51.
807 <https://doi.org/10.1016/j.tca.2011.01.010>.
- 808 [28] S.C. Silvério, O. Rodríguez, J.A. Teixeira, E.A. Macedo, The Effect of Salts on the
809 Liquid–Liquid Phase Equilibria of PEG600 + Salt Aqueous Two-Phase Systems,
810 *J. Chem. Eng. Data* 58 (2013) 3528–3535. <https://doi.org/10.1021/jc400825w>.
- 811 [29] R. Sadeghi, F. Jahani, Salting-In and Salting-Out of Water-Soluble Polymers in
812 Aqueous Salt Solutions, *J. Phys. Chem. B* 116 (2012) 5234–5241.
813 <https://doi.org/10.1021/jp300665b>.
- 814 [30] F.A. e Silva, J.F.B. Pereira, K.A. Kurnia, S.P.M. Ventura, A.M.S. Silva, R.D.
815 Rogers, J.A.P. Coutinho, M.G. Freire, Temperature dependency of aqueous
816 biphasic systems: an alternative approach for exploring the differences between
817 Coulombic-dominated salts and ionic liquids, *Chemical Communications* 53
818 (2017) 7298–7301. <https://doi.org/10.1039/C7CC02294H>.
- 819 [31] Y. Chen, J. Ryu, J.D. Bazak, D.T. Nguyen, K.S. Han, Z. Li, J.Z. Hu, K.T. Mueller,
820 V. Murugesan, Ion Solvation-Driven Liquid–Liquid Phase Separation in Divalent
821 Electrolytes with Miscible Organic Solvents, *The Journal of Physical Chemistry C*
822 127 (2023) 15443–15453. <https://doi.org/10.1021/acs.jpcc.3c01701>.
- 823 [32] S. Großhans, G. Wang, J. Hubbuch, Water on hydrophobic surfaces: mechanistic
824 modeling of polyethylene glycol-induced protein precipitation, *Bioprocess Biosyst.*
825 *Eng.* 42 (2019) 513–520. <https://doi.org/10.1007/s00449-018-2054-5>.
- 826 [33] A.M. Azevedo, A.G. Gomes, P.A.J. Rosa, I.F. Ferreira, A.M.M.O. Pisco, M.R.
827 Aires-Barros, Partitioning of human antibodies in polyethylene glycol–sodium
828 citrate aqueous two-phase systems, *Sep. Purif. Technol.* 65 (2009) 14–21.
829 <https://doi.org/10.1016/j.seppur.2007.12.010>.
- 830 [34] N. Saha, B. Sarkar, K. Sen, Aqueous biphasic systems: A robust platform for
831 green extraction of biomolecules, *J. Mol. Liq.* 363 (2022) 119882.
832 <https://doi.org/10.1016/j.molliq.2022.119882>.
- 833 [35] X. Wang, T. Guo, Y. Shu, J. Wang, The anion of choline-based ionic liquids
834 tailored interactions between ionic liquids and bovine serum albumin, MCF-7 cells,
835 and bacteria, *Colloids Surf. B Biointerfaces* 206 (2021) 111971.
836 <https://doi.org/10.1016/j.colsurfb.2021.111971>.
- 837 [36] L. Xue, Y. Zhao, L. Yu, Y. Sun, K. Yan, Y. Li, X. Huang, Y. Qu, Choline acetate
838 enhanced the catalytic performance of *Candida rugosa* lipase in AOT reverse
839 micelles, *Colloids Surf. B Biointerfaces* 105 (2013) 81–86.
840 <https://doi.org/10.1016/j.colsurfb.2012.12.050>.
- 841 [37] R. Raoufinia, A. Mota, S. Nozari, L. Aghebati Maleki, S. Balkani, J. Abdolalizadeh,
842 A methodological approach for purification and characterization of human serum
843 albumin, *J. Immunoassay Immunochem.* 37 (2016) 623–635.
844 <https://doi.org/10.1080/15321819.2016.1184163>.
- 845 [38] J. Michałowicz, Bisphenol A – Sources, toxicity and biotransformation, *Environ.*
846 *Toxicol. Pharmacol.* 37 (2014) 738–758.
847 <https://doi.org/10.1016/j.etap.2014.02.003>.
- 848 [39] X. Liu, L.-R. Zhao, S.-H. Sang, Y.-Y. Gao, Q. Ge, Mean Ionic Activity Coefficients
849 of NaBr in the Ternary System NaBr–SrBr₂–H₂O at 288.15 K using the Cell
850 Potential Method, *J. Chem. Eng. Data* 65 (2020) 5083–5089.
851 <https://doi.org/10.1021/acs.jced.9b01137>.

- 852 [40] X. Xie, X. Wang, X. Xu, H. Sun, X. Chen, Investigation of the interaction between
853 endocrine disruptor bisphenol A and human serum albumin, *Chemosphere* 80
854 (2010) 1075–1080. <https://doi.org/10.1016/j.chemosphere.2010.04.076>.
- 855 [41] J. Martosella, N. Zolotarjova, H. Liu, G. Nicol, B.E. Boyes, Reversed-Phase High-
856 Performance Liquid Chromatographic Prefractionation of Immunodepleted
857 Human Serum Proteins to Enhance Mass Spectrometry Identification of Lower-
858 Abundant Proteins, *J. Proteome Res.* 4 (2005) 1522–1537.
859 <https://doi.org/10.1021/pr050088l>.
- 860 [42] L.N. Vandenberg, I. Chahoud, J.J. Heindel, V. Padmanabhan, F.J.R.
861 Paumgartten, G. Schoenfelder, Urinary, Circulating, and Tissue Biomonitoring
862 Studies Indicate Widespread Exposure to Bisphenol A, *Environ. Health Perspect.*
863 118 (2010) 1055–1070. <https://doi.org/10.1289/ehp.0901716>.
- 864 [43] Dhanjai, A. Sinha, L. Wu, X. Lu, J. Chen, R. Jain, Advances in sensing and
865 biosensing of bisphenols: A review, *Anal. Chim. Acta* 998 (2018) 1–27.
866 <https://doi.org/10.1016/j.aca.2017.09.048>.
- 867 [44] K.A. Thayer, D.R. Doerge, D. Hunt, S.H. Schurman, N.C. Twaddle, M.I.
868 Churchwell, S. Garantziotis, G.E. Kissling, M.R. Easterling, J.R. Bucher, L.S.
869 Birnbaum, Pharmacokinetics of bisphenol A in humans following a single oral
870 administration, *Environ. Int.* 83 (2015) 107–115.
871 <https://doi.org/10.1016/j.envint.2015.06.008>.
- 872 [45] F. Pena-Pereira, W. Wojnowski, M. Tobiszewski, AGREE—Analytical
873 GREENness Metric Approach and Software, *Anal. Chem.* 92 (2020) 10076–
874 10082. <https://doi.org/10.1021/acs.analchem.0c01887>.
- 875 [46] W. Wojnowski, M. Tobiszewski, F. Pena-Pereira, E. Psillakis, AGREEprep –
876 Analytical greenness metric for sample preparation, *TrAC Trends in Analytical
877 Chemistry* 149 (2022) 116553. <https://doi.org/10.1016/j.trac.2022.116553>.
- 878 [47] R. González-Martín, A. Gutiérrez-Serpa, V. Pino, M. Sajid, A tool to assess
879 analytical sample preparation procedures: Sample preparation metric of
880 sustainability, *J. Chromatogr. A* 1707 (2023) 464291.
881 <https://doi.org/10.1016/j.chroma.2023.464291>.
- 882 [48] N. Manousi, W. Wojnowski, J. Płotka-Wasyłka, V. Samanidou, Blue applicability
883 grade index (BAGI) and software: a new tool for the evaluation of method
884 practicality, *Green Chemistry* 25 (2023) 7598–7604.
885 <https://doi.org/10.1039/D3GC02347H>.
- 886 [49] H. Passos, A.C.A. Sousa, M.R. Pastorinho, A.J.A. Nogueira, L.P.N. Rebelo, J.A.P.
887 Coutinho, M.G. Freire, Ionic-liquid-based aqueous biphasic systems for improved
888 detection of bisphenol A in human fluids, *Analytical Methods* 4 (2012) 2664–2667.
889 <https://doi.org/10.1039/c2ay25536g>.
- 890 [50] C. Polesca, H. Passos, A.C.A. Sousa, N.M. Tue, J.A.P. Coutinho, T. Kunisue,
891 M.G. Freire, Sustainable pretreatment of blood samples using hydrophobic
892 eutectic solvents to improve the detection of bisphenol A, *Green Chemistry* 27
893 (2025) 200–208. <https://doi.org/10.1039/D4GC03396E>.
- 894 [51] Á.I. López-Lorente, F. Pena-Pereira, S. Pedersen-Bjergaard, V.G. Zuin, S.A.
895 Ozkan, E. Psillakis, The ten principles of green sample preparation, *TrAC Trends
896 in Analytical Chemistry* 148 (2022) 116530.
897 <https://doi.org/10.1016/j.trac.2022.116530>.
- 898

Highlights

- Polypropylene glycol with cholinium or sodium salts forms ABS for serum protein depletion.
- Salt selection tunes ABS phase behavior, protein partition, and BPA recovery.
- Protein depletion is achieved via *interphase precipitation* or *bottom phase retention*.
- *Interphase precipitation* delivers optimal protein depletion and BPA recovery.
- ABS enables accurate detection for exposure and bioanalytical applications.

Declaration of interests

The authors declare that they have no known competing financial interests or personal relationships that could have appeared to influence the work reported in this paper.

The authors declare the following financial interests/personal relationships which may be considered as potential competing interests:

Journal Pre-proof